Geophys. J. Int. (2002) **149,** 313–327

Anisotropy beneath California: shear wave splitting measurements using a dense broadband array

J. Polet and H. Kanamori

Seismological Laboratory, Caltech, Pasadena, CA 91125, *USA. E-mail: polet@gps.caltech.edu*

Accepted 2001 October 10. Received 2001 October 1; in original form 2001 March 16

SUMMARY

We have determined the shear wave splitting parameters for a dense network of broad-band stations in the western United States using high-quality *SKS* and *SKKS* waveforms, with particularly high spatial resolution in the southern California region covered by the TriNet seismic network. The alignment of most fast polarization directions can be explained by plate-tectonic, extensional and compressional events. We find that the overall pattern of fast directions agrees well with the P_n anisotropy model by Hearn that images the uppermost mantle. Furthermore, the measured fast directions are generally orthogonal to the maximum horizontal compressive stress directions as determined from shallow crustal stress indicators (World Stress Map). This suggests that the pattern of anisotropy in the western US is predominantly uniform throughout the crust and upper mantle and that a 100–150 km thick layer (as estimated from the *SKS* delay time, assuming 4 per cent anisotropy) of anisotropic material has experienced coherent strain conditions and has undergone a similar deformation history. A more detailed investigation reveals small-scale lateral variations in anisotropy that are manifested by minor differences in splitting parameters between closely located stations as well as between *SKS* and *SKKS* for the same station-event pairs. We also identify a contrast in splitting parameters between central (the greater Bay area) and southern California. In central California, our measurements show evidence for variation of splitting parameters with backazimuth, while in southern California the pattern of measurements can be fit adequately with a single-layer anisotropy model. This contrast dominates any consistent effect of the San Andreas Fault (SAF). We can fit the variation of splitting parameters as a function of polarization azimuth for some stations in the vicinity of the SAF better with a two-layer anisotropy model than a single layer model, with one thin layer having a fast direction parallel to the SAF. However, many alternative models, which could incorporate dipping axes of anisotropy, lateral variation of anisotropy or a more continuous variation of fast direction with depth, would be able to produce a similar fit.

Key words: anisotropy, continental margin, *S* waves, shear-wave splitting, stress distribution.

INTRODUCTION

Shear wave splitting parameters obtained from teleseismic *S* waves can be used to examine the seismic anisotropy of a region and the related history of deformation. Measurements of anisotropy are one of the few tools available to seismology that can tell us about the current or past dynamics of the interior of the Earth, especially the upper mantle (Kind *et al.* 1985; Silver & Chan 1991). California, in particular, is an interesting region because of its complex plate tectonic history. The western United States is also one of the most densely instrumented regions in the world, enabling a detailed investigation of the local anisotropic parameters and their geographical variation.

Our main interest is in obtaining high-quality measurements of shear wave splitting from teleseismic *SKS* and *SKKS* waves, and establishing the lithospheric and asthenospheric pattern of anisotropy. We also would like to examine the relationship between this pattern and the shallow measurements of stress that have been performed over recent years. This study extends earlier works by Savage & Silver (1993), Ozalaybey & Savage (1994, 1995) (Ozalaybey & Savage (1995) referred to as OS95 hereafter) and Liu *et al.* (1995) by adding many more station-event pairs. We used very strict criteria in our *SKS* and *SKKS* data selection, and chose not to use any other phases, because of possible contamination from the source side of the path and, in the case of *S* phases with large turning depths, interaction with D''. We consider lateral variations of anisotropy, as well as variations with depth such as two-layered anisotropic models. The previous studies found evidence for alignment of the fast direction of anisotropy in California in a direction parallel to the San Andreas fault

(SAF-parallel anisotropy) in the crust and upper mantle, as well as a deeper EW-oriented fast direction (EW-fast anisotropy). This latter feature has been interpreted as being a result of the asthenospheric flow in the slabless window left behind the Farallon plate (OS95).

METHOD AND DATA

The method we use for estimating the fast polarization angle and delay time is described in detail in Silver & Chan (1991). Since the incidence angle of the phases used in this study is nearly vertical, we assume that the *S*-wave particle motion is on a horizontal plane. For the anisotropic media explored here, the *S*-wave velocity is a function of its polarization angle on this horizontal plane. This anisotropy causes the shear wave to split into two phases, one with a polarization azimuth in the fast direction (ϕ), measured clockwise from north and another with a perpendicular polarization azimuth, that exhibit an arrival time difference (δt). The splitting parameters (ϕ, δt) can be determined by finding the ϕ and δt that, when used to correct the observed seismograms for the anisotropy, most completely remove the splitting. In cases where the isotropic polarization angle ϕ_p (the angle between north and the polarization direction) is predicted to be equal to the backazimuth (ϕ_b) of the ray, such as with *SKS*, *SKKS* and *PKS* phases (we will denote these phases by **KS*), we can estimate the splitting parameters to be those that minimize the energy on the transverse component. To obtain these optimal values we tested all possible values of ϕ with increments of 1° and values of δt ranging between 0 and 4 s with increments of 0.05 or 0.10 s. Fig. 1 illustrates this procedure for *SKS* waveforms from an event recorded at station GSC.

For all types of *S* phases, the splitting parameters can also be determined by finding the ϕ and δt that minimize the smaller eigenvalue of the 2-D covariance matrix of the corrected horizontal particle motion. This second method is equivalent to finding the most linear

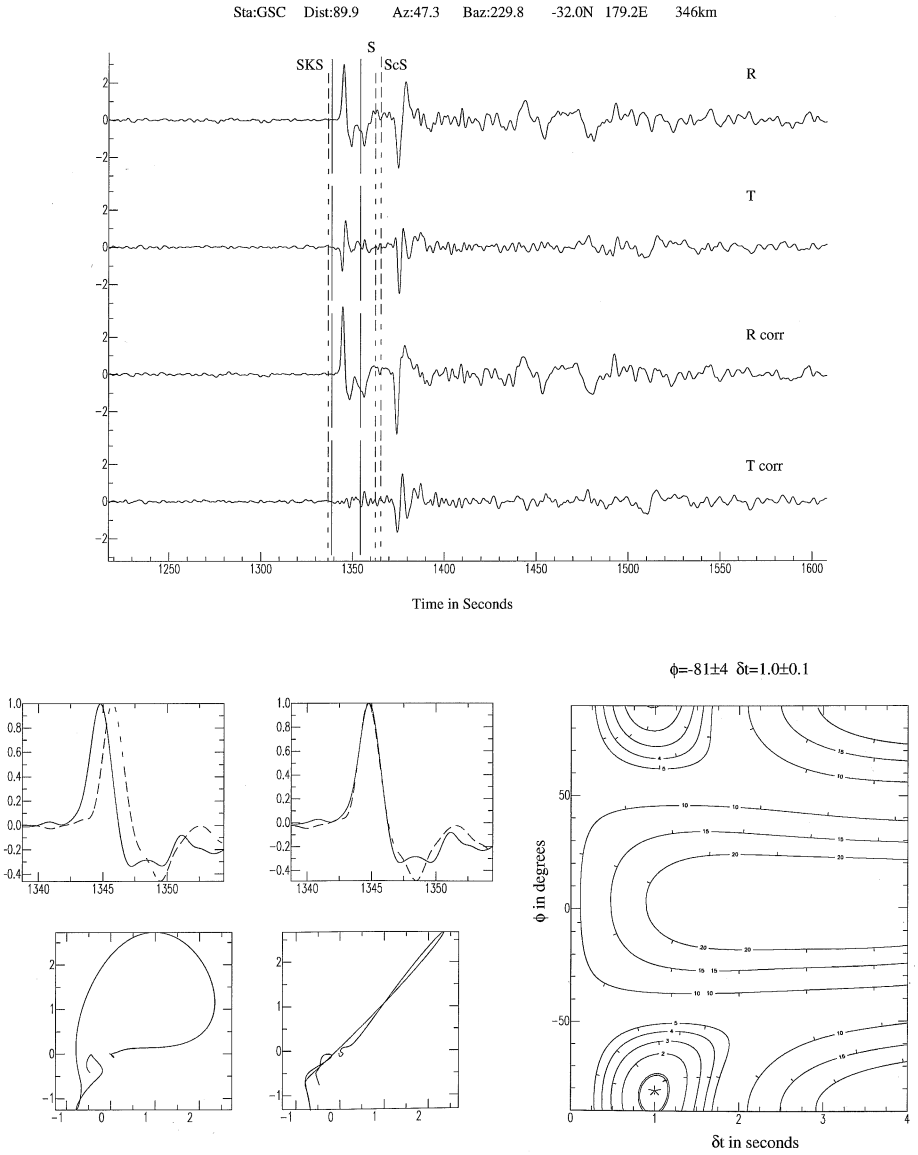

Figure 1. Top: top two traces, the original horizontal components. Bottom two traces, the horizontal components corrected for the determined values of ϕ and δt. Note that in the corrected seismograms the energy arriving on the transverse component has been removed. Bottom left: top two panels, superposition of fast and slow components uncorrected (left) and corrected for the delay time (right). Note the great similarity in the waveforms. Bottom two panels, horizontal particle motion for uncorrected (left) and corrected (right) components. Bottom right: contour plot of the energy on the transverse component in (ϕ, δt) space. Minimum value is shown as star with 95 per cent confidence region (double contour) and multiples of that contour level.

particle motion. By applying this method to $^*KS$ phases, we can allow for the possibility that energy on the transverse component is caused by the deviation of the ray away from the great-circle path (e.g. by a dipping layer) or by misorientation of the horizontal components. From this procedure we also obtain an estimate of ϕ_p. The uncertainties are determined for all individual measurements as in Silver & Chan (1991). When splitting measurements for $^*KS$ phases can be obtained using both procedures, we chose the measurement with the smallest error.

Measurements that have error ellipses that are narrow in the ϕ direction, but elongated in the δt direction, suggest little or no splitting. Such measurements are called 'nulls' and are consistent with either isotropic material or with ϕ perpendicular to or along the polarization direction. We regarded individual splitting measurements as reliable only if they satisfied the following criteria: (1) there was a strong similarity between the waveforms of the fast and slow component; (2) the error ellipse was well constrained; (3) the uncorrected particle motion was clearly elliptical; and (4) we obtained consistent results using slightly different time windows and using both procedures for estimating δt and ϕ for $^*KS$ phases.

Our data set consists of TriNet, Anza, Berkeley and United States National Seismic Network broad-band recordings of *SKS* and *SKKS* phases, mainly from deep events along the western Pacific rim. Previous authors (Savage & Silver 1993; OS95; Liu *et al.* 1995) have examined a subset of this data. We have reanalysed (and reinterpreted) some of these data, and added a substantial new data set from more events and newly installed stations. Stations of these four networks (Appendix A) form a dense seismic array that is ideally suited for the investigation of lateral variations of anisotropy. The volume of this data set provides convincing evidence for shear wave splitting as being caused by anisotropy rather than lateral structural inhomogeneities over a wide geographical area.

For many of these stations we obtained high-quality data for only a small number of events, because of data availability problems with the USNSN and Anza networks or because the station in question had only been active for a short time period (TriNet). However, part of the TriNet network has been active for over a decade as the TERRAscope network. These stations give a good azimuthal coverage, and thus can be used as 'calibration points'. We will assume in our interpretation that if a well-covered station shows no variation of splitting parameters with backazimuth, nearby stations with consistent, but fewer, measurements probably also behave in a simple manner.

Because we use teleseismic *S*-phases, we can obtain only a limited depth resolution for the anisotropy. Studies of local shallow *S* waves in southern California at a depth of 15 km and shallower suggest that anisotropy in this part of the crust is limited to a delay time of about 0.2 s or less (Li *et al.* 1994). Resolution of depth-dependent anisotropy for greater depths can be gained by comparing the splitting parameters measured at adjacent stations.

To illustrate the quality and coverage of the data, Figs 2(a) and (b) show the transverse component of the waveform data we collected for a deep event near Fiji, before and after correction for anisotropy using our measurements of fast direction and delay time. The velocity traces were filtered with a Butterworth bandpass filter between 1 and 100 s to eliminate the long-period noise at some stations. The *SKS* arrival, which is obvious on the original transverse component for most stations (left-hand panels in Fig. 2), is removed by the correction for splitting (right-hand panels). For some stations minor scattered secondary arrivals are still seen, as would be expected.

Table 1. Events used in this study.

Event origin time	Latitude	Longitude	Depth (km)	Moment magnitude
08/06/88 00:36:24	25.19	94.89	100.5	7.2
09/16/89 02:05:06	40.10	52.17	34.5	6.4
03/21/90 16:46:06	−30.71	−179.38	157.3	6.6
04/26/90 09:37:14	36.01	100.27	15.0	6.3
01/25/91 17:38:38	−1.72	139.11	15.0	6.1
10/19/91 21:23:15	30.22	78.24	15.0	6.8
04/03/92 03:19:52	−5.66	151.51	34.0	6.5
08/02/92 12:03:20	−7.27	121.83	498.3	6.6
08/19/92 02:04:36	42.19	73.32	17.0	7.2
05/18/93 10:19:38	19.97	122.65	188.2	6.7
08/07/93 00:00:37	26.68	125.84	164.9	6.4
09/29/93 11:16:04	0.62	121.70	88.9	6.3
10/02/93 08:42:32	38.16	88.82	15.0	6.1
10/13/93 02:06:00	−6.04	146.11	15.0	6.9
04/18/94 17:29:56	−6.61	154.92	52.1	6.7
02/05/95 22:51:10	−37.61	179.40	15.0	7.1
02/17/96 05:59:29	−0.67	136.62	15.0	8.2
06/11/96 18:22:55	12.74	125.41	28.5	7.1
06/17/96 11:22:18	−7.38	123.02	584.2	7.8
09/05/96 23:42:06	21.78	121.45	30.8	6.8
04/23/97 19:44:28	13.83	145.05	95.1	6.5
05/03/97 16:46:02	−31.70	−179.06	119.3	6.9
05/25/97 23:22:33	−32.02	−179.95	345.0	7.1
09/04/97 04:23:37	−26.45	178.52	621.0	6.8
04/20/99 19:04:08	−31.79	−178.79	104.4	6.5
06/14/00 02:15:25	−25.45	178.38	615.4	6.4
08/15/00 04:30:08	−31.42	−179.95	367.4	6.6

The other events used in this study (Table 1) have the same data quality as shown in Fig. 2. Many of the selected events have large source depths (>50 km) that enhance the sharpness and signal-to-noise ratio of the phase arrivals. Unfortunately, no waveform data for events in the range of backazimuths between 20° and 180° produced reliable splitting parameters.

At two stations (ISA and MLAC) we could not determine any high-quality splitting measurements, even when taking into account a possible rotation of the $^*KS$ arrivals with respect to the backazimuth or misorientation of the horizontal components of the sensor. These two stations are located above two of the greatest known velocity anomalies in the western United States, namely the Isabella anomaly (e.g. Raikes 1978) and the Mammoth Lakes Volcanic region, respectively. We believe that these lateral heterogeneities in the upper mantle cause sufficient waveform complexity to render reliable anisotropy measurements impossible. For all other stations in Fig. 3, however, we obtained at least one high-quality *SKS* splitting measurement.

MEASUREMENTS

In Fig. 3 we show the fast polarization directions and delay times for the western US that we measured using *SKS* and *SKKS* data, by plotting arrows parallel to the fast directions and proportional in length to the delay times. We plotted splitting parameters in smaller regions and included station codes on the maps in Figs A1–A3 of Appendix A. In general, results from different events are consistent for most stations in southern California and the eastern part of our study area. On our maps, we do not show one single set of 'average' splitting parameters for every station, because we believe there are resolvable (although in most cases small) variations in splitting

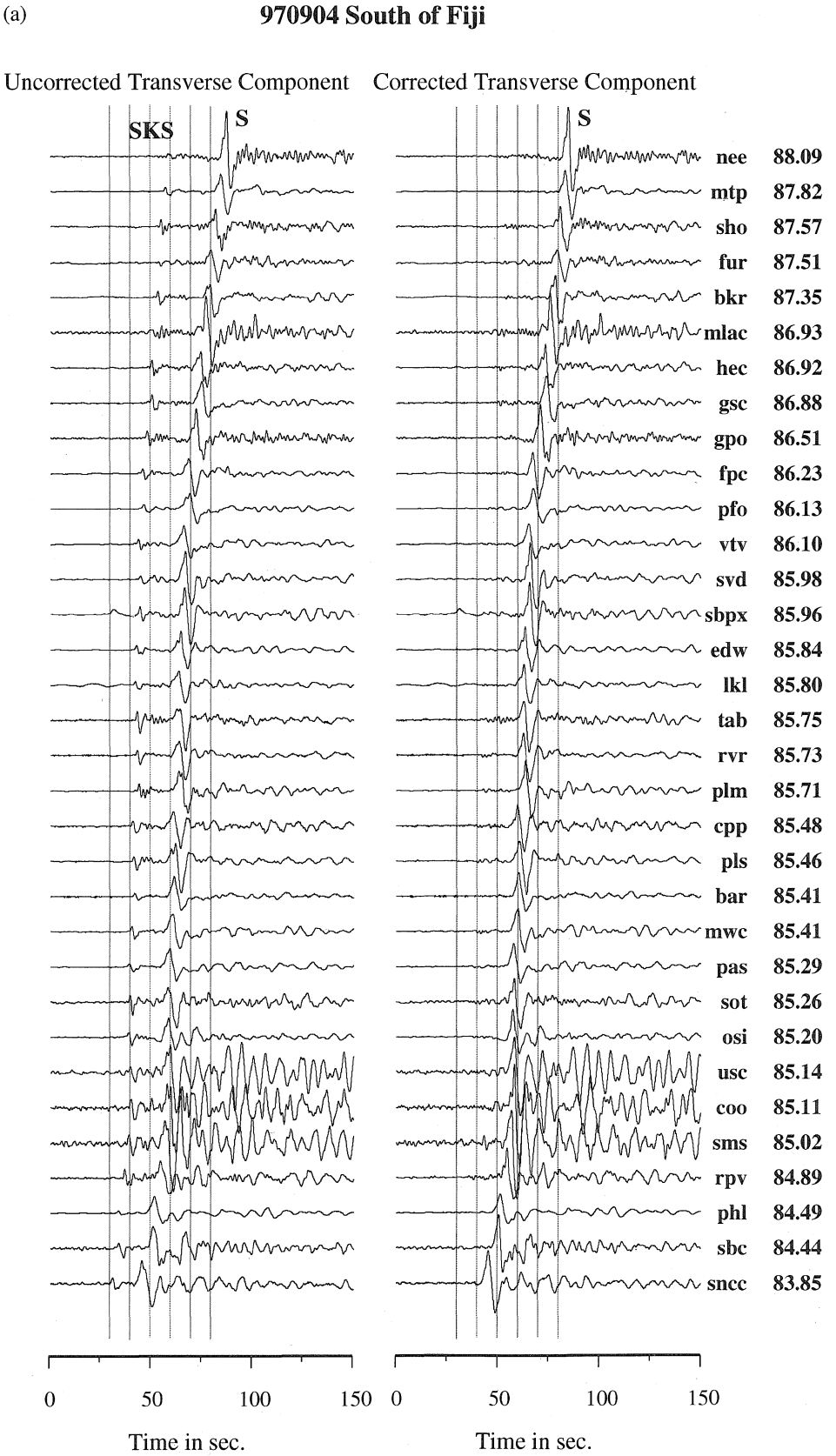

Figure 2. (a) Record section of original (left) and corrected (right) transverse components for a deep event near Fiji, recorded by TriNet. Numbers to the right of the traces give the epicentral distance in degrees. The large amplitude arrival is direct *S*-wave, preceded by a distinct *SKS* arrival on the transverse component on the left. Traces are aligned on the origin time of the event. Also note the change in the *S* waveform after the correction. (b) As in (a) for the Berkeley, Anza and USNSN network stations (from top to bottom).

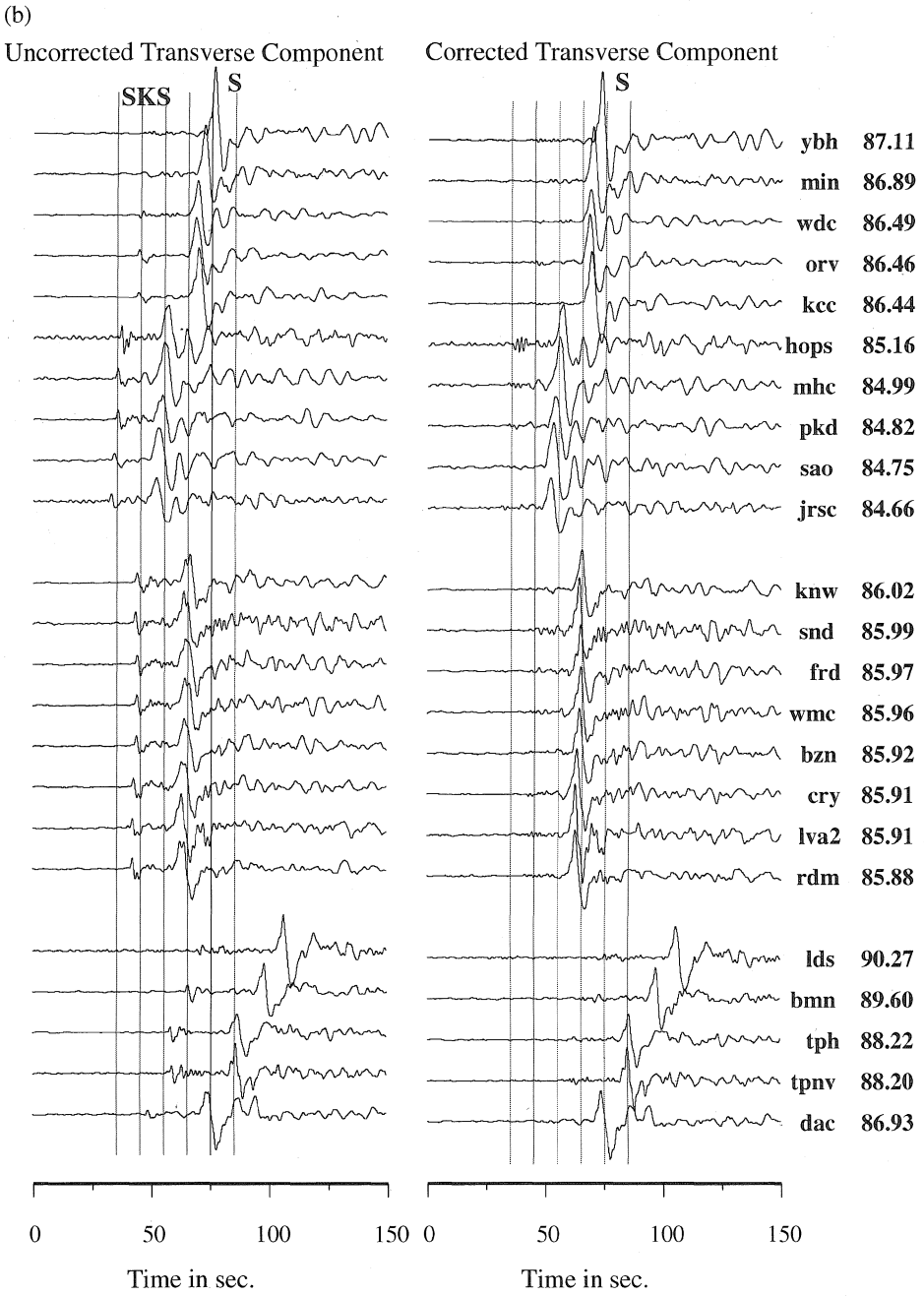

Figure 2. (*Continued.*)

parameters with polarization azimuth and angle of incidence. The existence of these variations implies that if average values are used in a correction for receiver-side anisotropy (as in the detection and estimation of transverse isotropy near the core–mantle boundary using *S* phases), significant errors in the analysis may result, which in many cases can be avoided by choosing the most appropriate, instead of the average, splitting parameters.

THE BIG PICTURE

Fig. 3 shows a contrast between the splitting parameters in northern California (mostly Berkeley network data) and southern California (mostly TriNet data). The southern California measurements are very similar for different events, whereas some of the northern California measurements display a strong variation with backazimuth, especially in delay times (as will be shown in more detail in a later section of this paper). In southern California west of the San Andreas fault and north of the Garlock fault, most stations show a consistent fast direction close to EW, with delay times varying between 0.75 and 1.5 s. This range of delay times implies a layer of anisotropic material 100–150 km thick if we assume 4 per cent anisotropy, a value thought to be typical for sheared mantle rock. A small crustal contribution may be included in this total delay time; studies of crustal anisotropy in this region suggest delay times of less than 0.1–0.3 s (Li *et al.* 1994). To further investigate the relationship between these anisotropic splitting parameters and the crustal stress, we plot our results together with the A and B quality measurements of maximum compressive stress direction from the World Stress

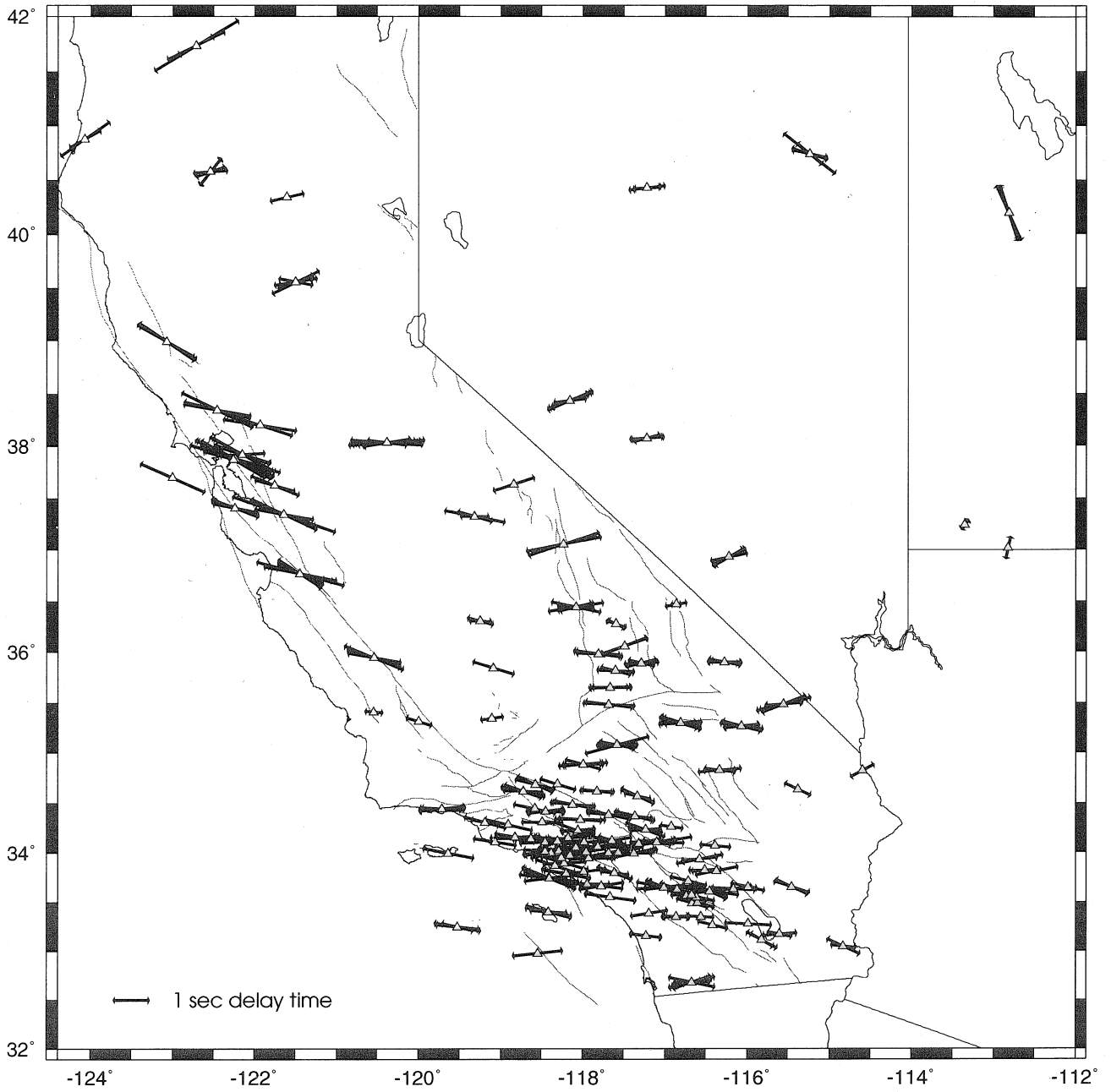

Figure 3. Map of all splitting measurements (from this study). Arrows are plotted on the station locations, their direction indicates fast direction and their length is proportional to delay time. Major California fault systems are also shown. More detailed maps including station names can be found in Appendix A.

Map (1997) in Fig. 4. These stress directions were mostly determined from borehole break-outs and focal mechanisms, and give an indication of the very shallow, crustal stress regime. Many studies of transpressional collision zones have found that the measured fast direction is aligned with the transpressional zone, orthogonal to the maximum compressive stress (e.g. McNamara *et al.* 1994; Silver *et al.* 1993; see Silver 1996, for an overview). Overall, we find that our fast directions are nearly orthogonal to the World Stress Map (WSM) vectors in central and southern California (Fig. 5). This suggests that the upper-mantle deformation in this area, as reflected by the splitting parameters, is consistent with the shallow stress indicators and implies that a 100–150 km thick layer of anisotropic material has experienced stress conditions in agreement with the surface measurements.

To further examine the depth dependence of the anisotropy in this area, we compare our results with the anisotropic P_n tomography from Hearn (1996). These P_n measurements sample only the uppermost mantle, whereas our *SKS* splitting measurements represent a vertical integral over the entire upper mantle and crust. These results should be consistent only when there are no large vertical variations in the orientation of anisotropy within the upper mantle. On visual inspection, the directions of P_n fast velocity correlate well with the *SKS* splitting fast directions, showing an EW-oriented fast velocity in southern and eastern California, and a more NW–SE striking fast direction in the Bay area. The direction of the fastest *P*-wave velocity in olivine, which is the main anisotropic mineral in the upper mantle, is aligned with its *a*-axis and the polarization direction of the fast *SKS* wave also coincides with this *a*-axis. Thus, the good

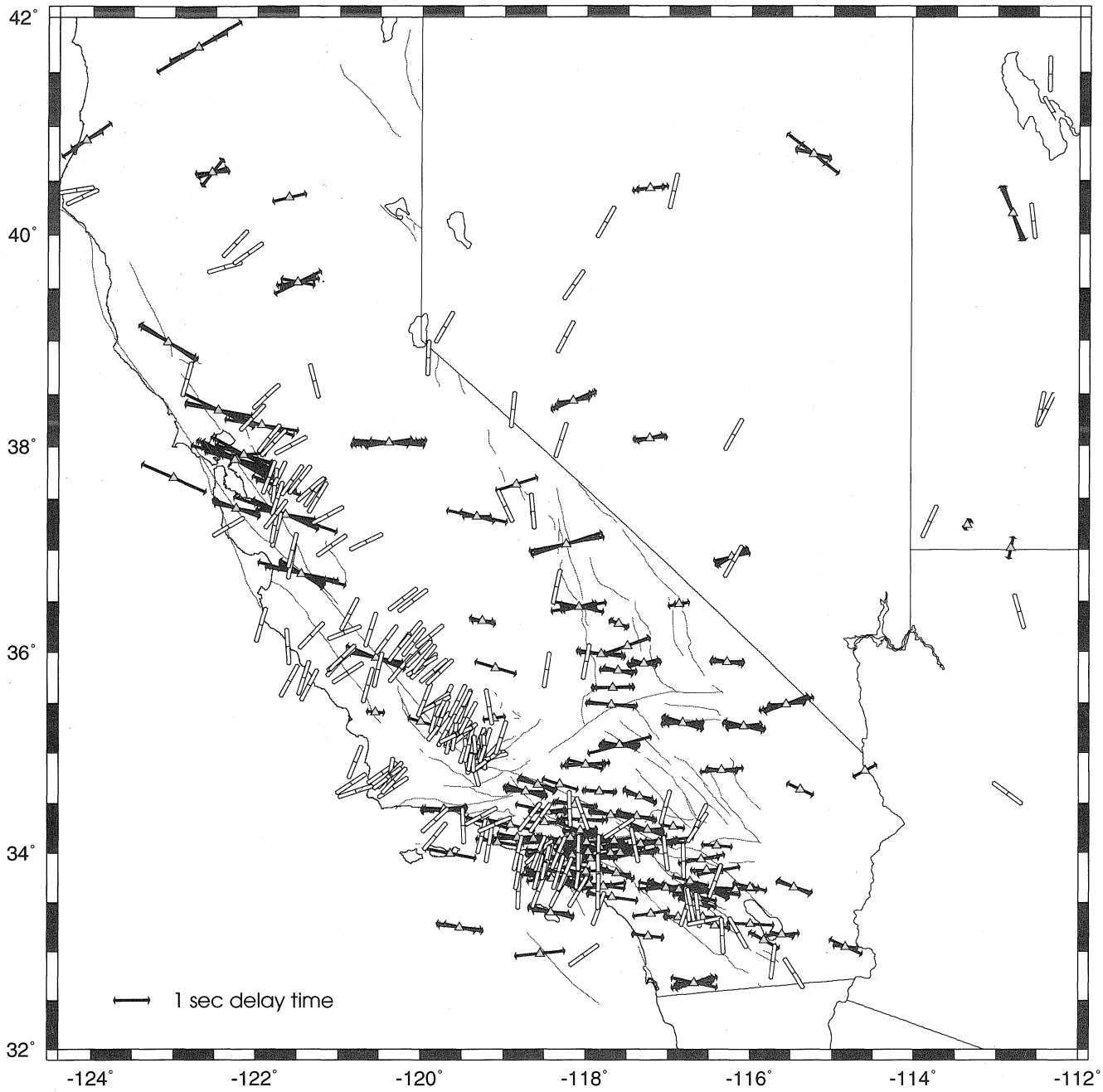

Figure 4. Map of splitting parameters and high-quality World Stress Map stress indicators. WSM stress indicators are plotted in white arrows in the direction of maximum horizontal compressive stress. Only A and B quality measurements are used.

correlation between these two measurements again suggests a coherent anisotropic pattern with depth.

In central California we find consistent splitting measurements at stations HOPS, BRIB, BKS, CVS, MHC, JRSC, SAO and PKD. The splitting parameters at these stations all exhibit strong variations with backazimuth/polarization direction. Interpretation of these measurements in terms of an anisotropic model is therefore less straightforward. Previous authors (e.g. Savage & Silver 1993; OS95) have focused on the proximity of these stations to the SAF to explain these variations; however, stations at similar distances from the SAF in southern California do not show this amount of variability in the splitting parameters, suggesting that it may be a regional effect, and not necessarily related to the SAF.

In southern California as well as the Sierra Nevada and the Mojave Desert, we find EW-oriented fast directions and delay times varying between 1 and 1.5 s. In the case of simple shear, a mineral will align its principal slip system with the direction of shear (Ribe 1989; Zhang & Karato 1995), since this requires the least energy. For olivine, the principal slip direction coincides with the *a*-axis and thus we would expect the fast polarization direction to orient in the direction of shear. In the case of California and the San Andreas Fault system, this mechanism would predict alignment of the fast direction with the SAF. The measured EW fast direction therefore suggests that shear at the plate boundary does not produce a dominant signal in the regional anisotropy. The EW orientation is, however, perpendicular to the direction of the late

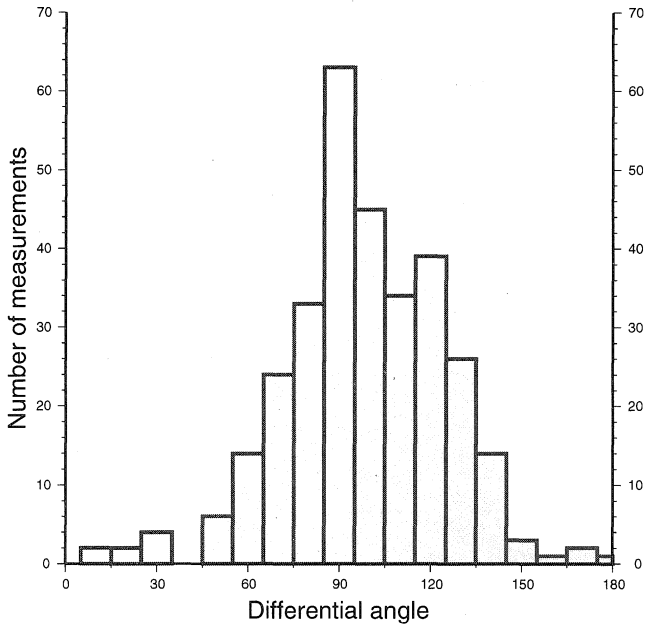

Figure 5. Histogram of the angle between the fast direction and the WSM maximum compressive stress direction, determined for every splitting measurement that has a WSM measurement within 50 km of its station location and measured clockwise from the fast polarization direction.

Cenozoic north–south compression in southern California (Liu *et al.* 1995), which in combination with the good agreement with the P_n and shallow stress measurements suggests a uniformly deforming crust and upper mantle in response to this compression. We cannot preclude that the fast direction could be a result of subduction of the Farallon plate, either because of the EW-directed shear induced on the asthenosphere beneath the continent (OS95), or remnant, frozen-in, anisotropy in the remnants of the Farallon plate under the North American plate. However, this hypothesis does not explain the consistency of the *SKS*, P_n and WSM directions in this area.

The orientation of the fast direction in northern California is parallel to the northeast subduction direction of the Gorda plate, which suggests that subduction-related deformation (NE–SW-directed internal shearing of the Gorda plate) may be responsible for the anisotropy observed at stations YBH, WDC and ARC, located north of 40° latitude. This interpretation agrees with that of (OS95), Hearn (1996) and Hartog & Schwartz (2000) for the same area.

The western Nevada stations show ENE–WSW fast directions, consistent with the observations made by Savage *et al.* (1990). This direction is inconsistent with both present-day extension (−60° to −80°) and the absolute plate motion (+55°). However, this fast direction can be interpreted as being a result of fossil anisotropy associated with pre-Miocene extension, of which the direction is about 68° (Savage *et al.* 1990) under the assumption that the *a*-axis of olivine aligns with the extension direction (Silver 1996).

DETAILED ANALYSIS

Regional patterns/separate station analysis

One diagnostic of particular interest is the variation of splitting parameters with backazimuth, especially for the data from stations close to the San Andreas Fault, which have been interpreted using

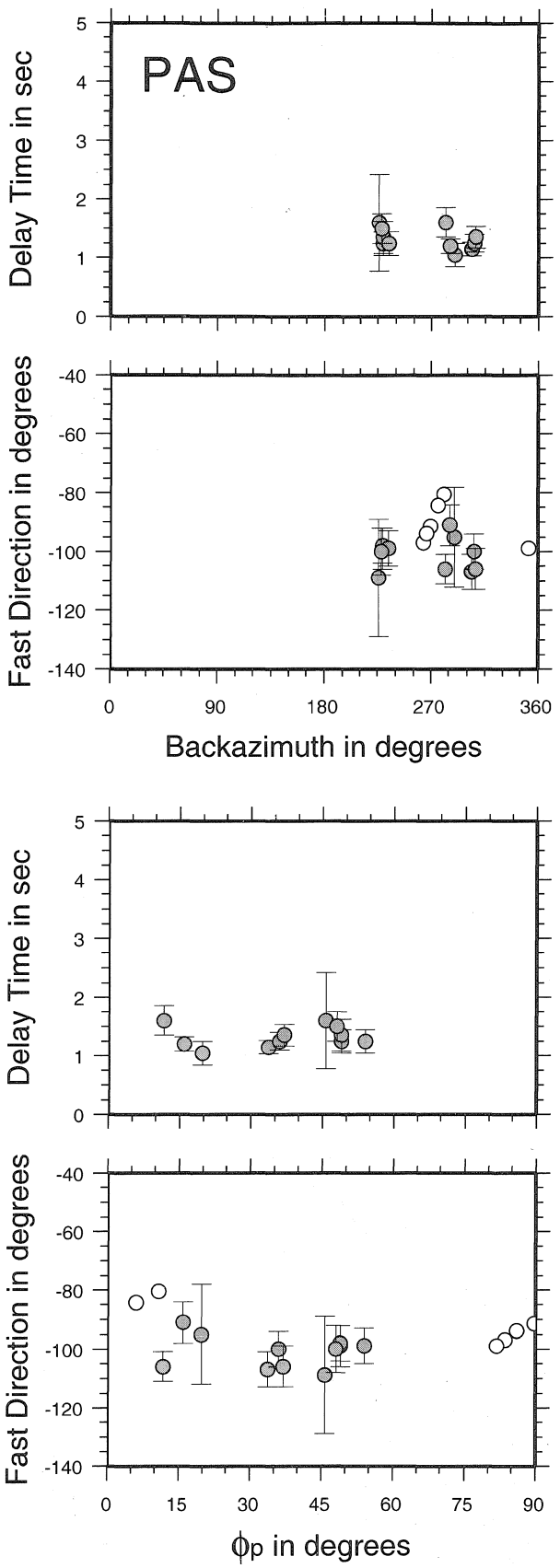

Figure 6. High-quality measurements of fast direction (ϕ) and delay time (δt) as a function of polarization direction (ϕ_p) modulo $\pi/2$ (bottom two panels) and backazimuth (top two panels) for station PAS. Open symbols represent null measurements.

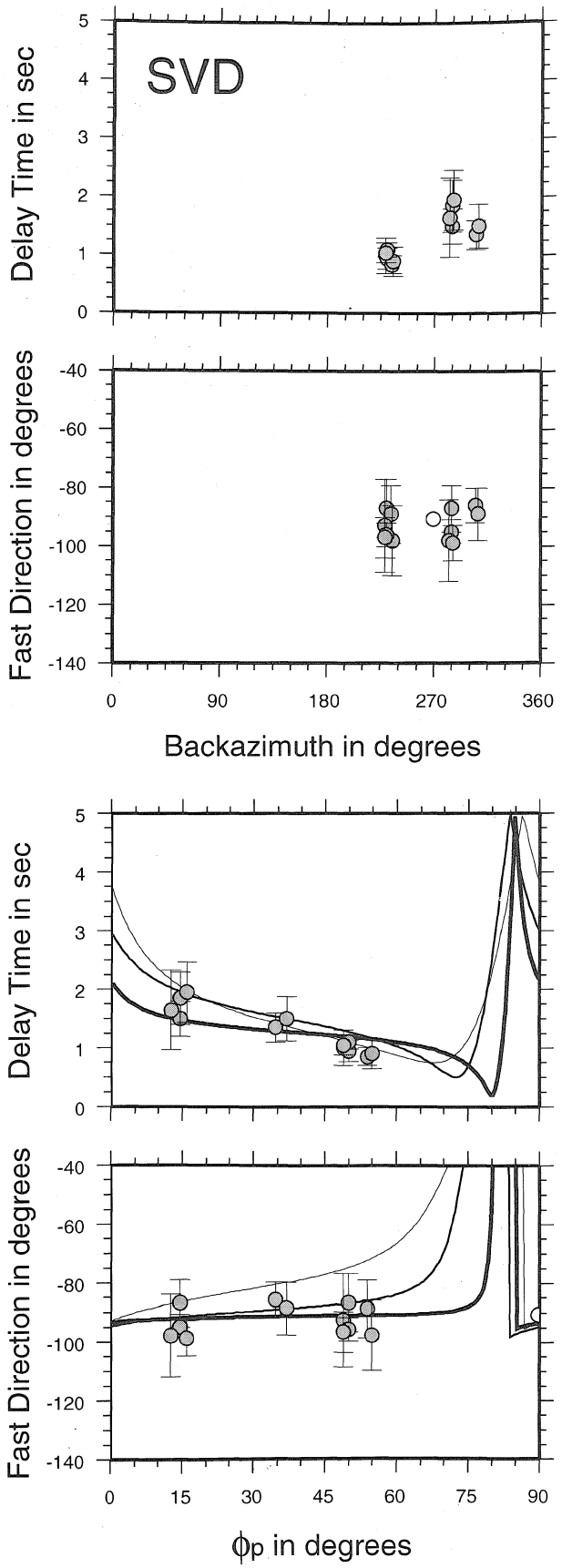

Figure 7. As Fig. 6, for station SVD. Curves in bottom left two panels correspond to two-layer models A (thinnest line), B and C (thickest line) in Table 2.

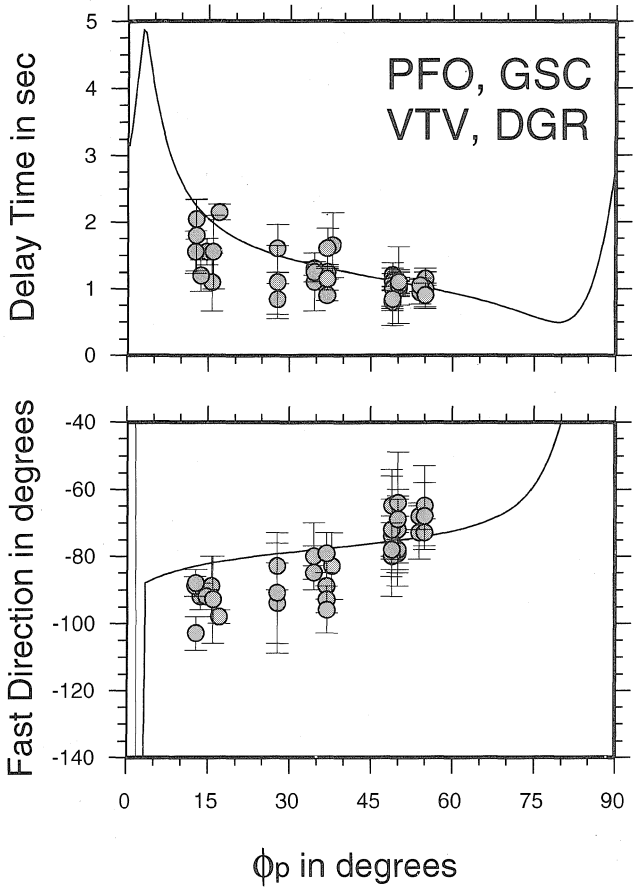

Figure 8. As Fig. 6, for the group of stations of PFO, GSC, DGR and VTV. Line shows predicted two-layer curves for model D in Table 2.

models of two-layer anisotropy (Savage & Silver 1993; Ozalaybey & Savage 1994, 1995). To investigate this variation closely, we reanalysed all events given in the table of OS95 for several key stations and added a significant new data set consisting of events since 1995. Several events from OS95 have been omitted from our measurements because of the low signal-to-noise ratio of the data, and/or poorly constrained splitting measurements. Of course, splitting measurements that display a variation with backazimuth do not necessarily have to be interpreted in terms of a two-layer model. Other authors have interpreted these types of measurements as being a result of a dipping symmetry axis of anisotropy (Hartog & Schwartz 2000), or lateral variation in anisotropy (Furlong 1998). In this paper we choose to interpret our data in terms of a two-layer model, and want to focus on making high-quality observations.

Station PAS is located in Pasadena, about 60 km from the San Andreas Fault (Appendix A). We show our $^*KS$ measurements of δt and ϕ for this station in Fig. 6 as a function of backazimuth, to demonstrate the event coverage, and also as a function of ϕ_p, modulo $\pi/2$. In the case of two anisotropic layers, we would expect the estimated splitting parameters to vary with $\pi/2$ periodicity as a function of ϕ_p (Silver & Savage 1994). Fig. 6 demonstrates that our measurements for station PAS show no sign of two-layer splitting. The measured fast direction is very consistent, and although there are some variations of delay time with ϕ_p, we do not attribute this variation to two-layer splitting because of the consistency in the fast direction. This delay time variation can be more easily explained in terms of small lateral variations in the strength of anisotropy, because

Table 2. Models of two anisotropic layers used in the study. The $(\phi_2, \delta t_2)$ and $(\phi_1, \delta t_1)$ values correspond to splitting pairs of the upper and lower layer, respectively.

Model	ϕ_1 (deg)	δt_1 (s)	ϕ_2 (deg)	δt_2 (s)
A	70	1.20	110	0.60
B	50	0.80	105	1.10
C	80	1.20	120	0.20
D	80	1.20	140	0.50
E	90	1.40	135	1.00
F	90	1.40	135	0.70

these rays do not sample exactly the same region. We conclude, in agreement with OS95, that this data can be interpreted with a single-layer, EW fast, anisotropy, with an average delay time of about 1.2 s. Several other stations for which data were available for a range of backazimuths showed similar results: USC, RPV, CMB and BAR fast directions and delay times displayed no significant variation with backazimuth.

TriNet station SVD (Fig. 7) is of particular interest because it is located almost on top of the San Andreas fault. The measurements for this station were modelled by OS95 using a two-layered model of anisotropy, partly based on the results for another nearby station, but, because of the small number of measurements, were interpreted as showing no fault-parallel anisotropy. The overall anisotropy at this site can be described as having an EW fast direction, with an average delay time of about 1.2 s, which is very similar to station PAS. Although there is a sizeable gap of about 30° in ϕ_p in our data coverage, the measurements show a comparable fast direction for all backazimuths. Delay times, however, seem to decrease consistently with polarization azimuth. We computed the curves for the two-layer models suggested by OS95, based on observations at stations PFO and LAC (models A and B, respectively, in Table 2), for a frequency of 0.1 Hz and included these in Fig. 7. We also include our own forward model (model C) to give an indication of the range of models that fit the data. A model with a thin layer on top of the overall pattern of EW aligned fast polarization direction and 1.20 s of delay time, explains the data slightly better than a model with a single layer. A thin, fault parallel, upper layer could represent the effect of finite strain associated with the plate motion between the North American and Pacific plates, its delay time of 0.30 s or less could reside in the crust.

Station PFO has been modelled in various papers with different results (Liu *et al.* 1995; OS95; Helffrich *et al.* 1994). In Fig. 8 we present the most complete data set yet, adding data from stations GSC, VTV and DGR, which show the same general trend. These stations show indications of two-layer splitting: a decrease of delay time and an increase in fast direction with increasing polarization azimuth. This general trend is fitted well by forward model D. A thin layer is added on top of the EW fast layer, which was used as a single-layer model to fit the stations in southwest California. The fast direction of this top layer is more or less parallel to the direction that would be predicted by shear associated with the SAF. However, since this model seems to fit the data of stations at distances greater than 100 km from the fault to the east, this variation in splitting parameters is not necessarily directly related to the San Andreas Fault system.

Another station for which OS95 suggested the presence of a two-layer model of anisotropy is station BKS of the Berkeley network (Fig. 9), also located close to the SAF at a distance of 40 km, in northern California. This station was modelled with an upper layer

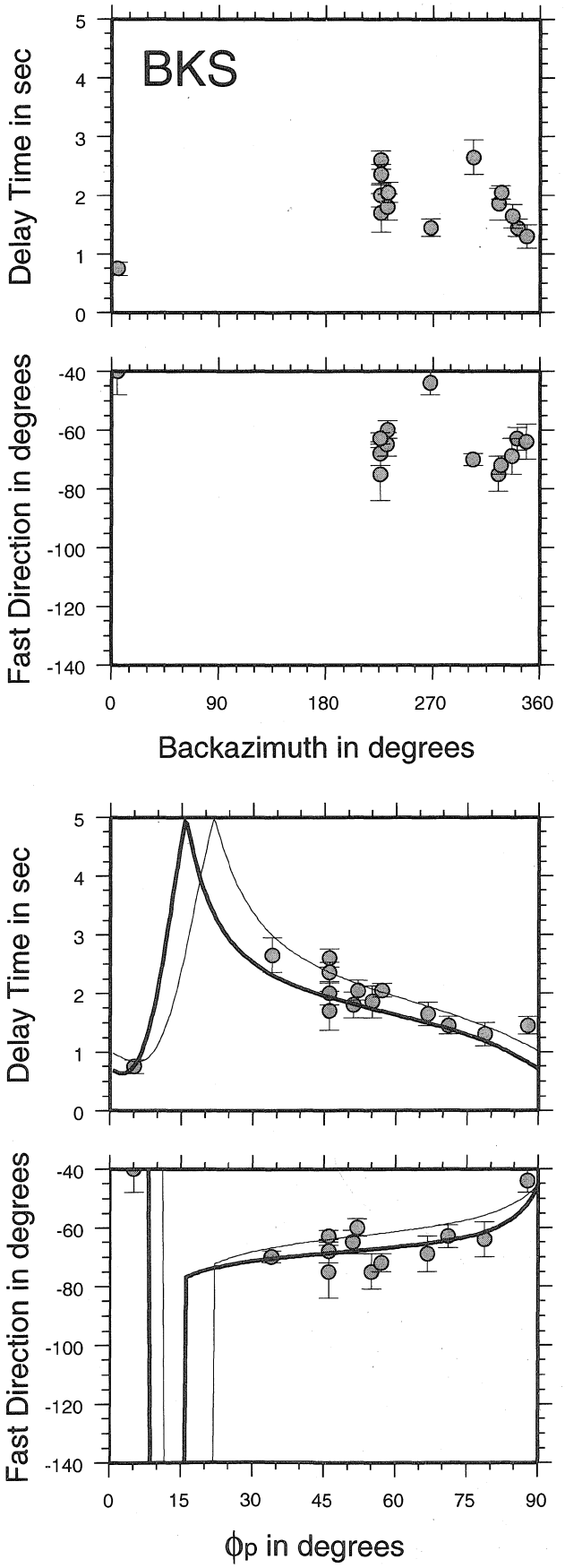

Figure 9. As Fig. 6 for Berkeley station BKS. Thin line shows curves predicted by model E, thick line for model F (both in Table 2).

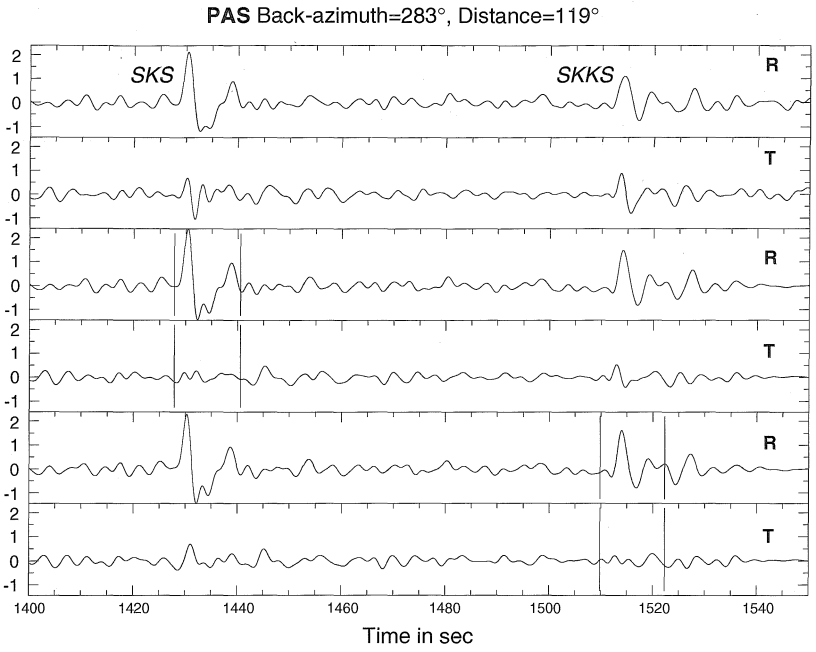

Figure 10. Top two traces, original radial and transverse seismograms. Middle two traces, radial and transverse seismograms after correction for *SKS* splitting. Bottom two traces, radial and transverse seismograms after *SKKS* splitting correction.

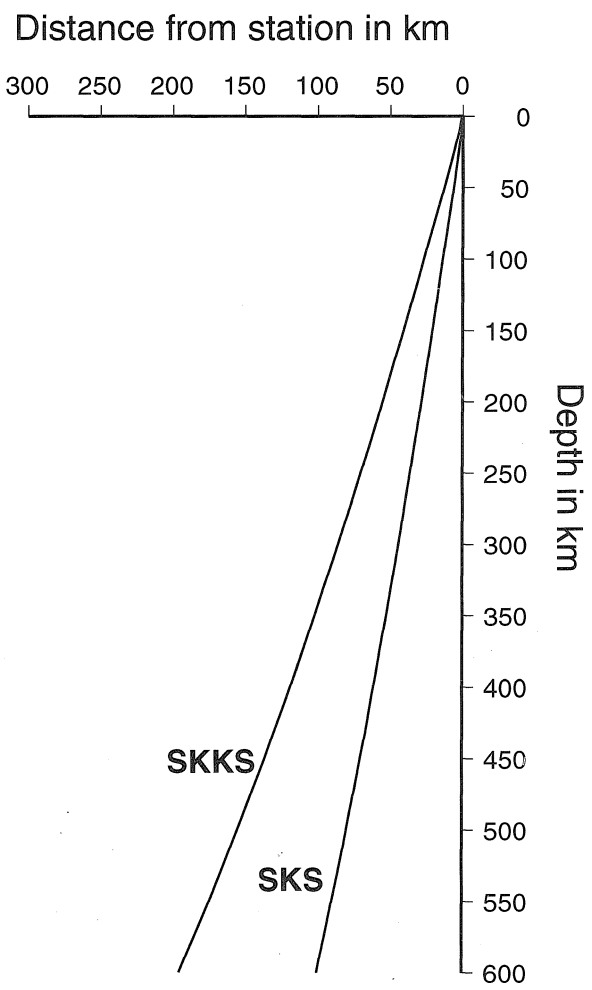

Figure 11. *SKS* and *SKKS* raypaths to station PAS for seismograms shown in Fig. 10.

with fast direction parallel to the local strike of the SAF and a delay time of 1.0 s, and a lower layer with EW fast direction and a delay time of 1.4 s. The measurements for this station are very similar to those of stations SAO, MHC, PKD, JRSC and HOPS, all located in the same region of California. A temporary network deployed in central California, close to station MHC, also shows results consistent with BKS (Hartog & Schwartz 2000). These stations all yield splitting parameters that are indicative of an anisotropic system that is more complicated than a simple one-layer model. Possible explanations for this more complex set of measurements include: a dipping symmetry axis (Hartog & Schwartz 2000), a double anisotropic layer system or a system of more complex vertically varying anisotropy (Rümpker & Silver 1998). The two-layer model suggested by OS95 seems to fit the data well (Fig. 9). This model consists of a lower layer with $\phi \sim 90° \pm 27°$ and $\delta t \sim 1.40 \pm 0.5$ s and an upper, fault parallel, layer of $\phi \sim 135 \pm 25$ and $\delta t \sim 1.00 \pm 0.50$ s. Because of the large number of free parameters in this inversion, the trade-offs between the model parameters are quite large. We found that a model with only a 0.70 s delay time in the upper layer could visually explain the data just as well (Fig. 9). The range of possible models is so large that using an inversion technique to solve for a detailed model of anisotropy is probably too ill-constrained for this type of data set; fitting the data with a physically realistic forward model is a more promising method to pursue.

SKS/*SKKS* VARIATION

Because of the high quality of this data set, we could detect small variations in measurements using *SKS* and *SKKS* for the same event, to investigate lateral heterogeneity in anisotropy. For a deep event near Sulawesi (Fig. 10), the *SKS* recorded at PAS produced measurements of $\phi \sim 77° \pm 12°$ and $\delta t \sim 0.95 \pm 0.25$ s, whereas the *SKKS* splitting parameters were determined as $\phi \sim 72° \pm 8°$ and $\delta t \sim 1.30 \pm 0.20$ s. These fast directions are consistent, but the difference in delay time is resolvable, as shown by the seismograms in Fig. 10. We attempted to determine the splitting parameters using

SKS and *SKKS* simultaneously, but found that the final result did not remove the transverse component for either phase. Station GSC shows a similar delay time difference between the two phases. Another event, near Flores, showed similar results. These results suggest that small variations of delay time with backazimuth, caused by lateral variations in the strength of anisotropy, should be expected, since the rays sample slightly different regions (Fig. 11). A similar conclusion can be drawn from the dense station coverage in Fig. 4: closely located stations show resolvable differences in anisotropic parameters.

CONCLUSIONS

We have determined shear wave splitting parameters for a dense network of stations in the western United States using high-quality *SKS* and *SKKS* waveforms. A comparison of fast polarization directions with shallow stress indicators as well as a P_n anisotropy model suggests that, for large parts of this area, the overall deformation pattern that causes this anisotropic fabric may be pervasive and consistent throughout the crust and upper mantle. Most fast directions we obtained in this study can be explained by current plate tectonic processes or are consistent with late Cenozoic compressional (southern California) or pre-Miocene extensional (Basin and Range) events. The range of measured delay times implies a layer of anisotropic material 100–200 km thick (under the assumption of 4 per cent anisotropy).

A detailed analysis of this data set reveals indications of depth-dependent anisotropy at some stations, and small but resolvable differences between *SKS* and *SKKS* splitting in single event-station pairs, indicating small-scale lateral variations. A marked contrast exists between the shear wave splitting parameters in central California and southern California. The southern California measurements, as a whole, are consistent for different events, whereas some of the central California measurements display a strong variation with backazimuth. Most apparent is this variation of splitting parameters for a group of stations in the greater Bay area; we can fit the fast directions and delay times measured at these stations with a two-layer model, the upper layer with a fast direction of 135° (from the north) and a delay time of 0.7 s, the bottom layer with an EW fast direction and a delay time of 1.40 s. This bottom layer could be connected to past subduction processes and the top layer is consistent with anisotropy aligned with shear on the SAF system. However, stations at similar distances from the SAF in southern California do not show this amount of complexity, suggesting that the variation in splitting parameters for the more northern stations may be a regional effect, and not necessarily related to the SAF. Furthermore, considering the number of free parameters involved and, accordingly, the large suite of anisotropy models that can explain these measurements, more constraints are needed and a more useful approach should include the construction of several realistic forward models, and directly comparing synthetic seismograms with the recorded waveform data.

Smaller variations in splitting parameters were seen for stations in southern California. For station SVD, located very close to the SAF, including a thin layer with fast direction parallel to the SAF, on top of a layer with an EW fast direction and a 1.2 s delay time, can explain the data slightly better than a model with a single layer. Another group of stations close to and east of the SAF shows indications of depth-dependent anisotropy. Again, this could be caused by a thin layer with a fast direction parallel to the SAF on top of a layer with EW-oriented fast direction, but since the lateral range of these stations extends to fairly great distances from the SAF, more events need to be analysed to determine the eastward limit of this anomaly. Measurements for most stations west of the SAF require only a consistent one-layer model, with minor lateral differences in the strength of anisotropy, as demonstrated by small but resolvable differences in delay times.

ACKNOWLEDGMENTS

We would like to thank Paul Silver for interesting discussions, and the use of his shear wave splitting codes. Thanks also go to Lianxing Wen for the use of his ray-tracing code. We would also like to thank John Vidale, two anonymous reviewers and Steven Ward for their suggestions to improve the manuscript.

REFERENCES

Furlong, K., 1998. Complex patterns of seismic anisotropy in regions of active tectonics, EGS Solicited Paper.

Hartog, R. & Schwartz, S.Y., 2000. Subduction-induced strain in the upper mantle east of the Mendocino triple junction, California, *J. geophys. Res.*, **105,** 7909–7930.

Hearn, T.M., 1996. Anisotropic P_n tomography in the western United States, *J. geophys. Res.*, **101,** 8403–8414.

Helffrich, G., Silver, P.G. & Given, H., 1994. Shear-wave splitting variation over short spatial scales on continents, *Geophys. J. Int.*, **119,** 561–573.

Kind, R., Kosarev, G.L., Makeyeva, L.I. & Vinnik, L.P., 1985. Observations of laterally inhomogenous anisotropy in the continental lithosphere, *Nature,* **318,** 358–361.

Li, Y.G., Teng, T. & Henyey, T.L., 1994. Shear wave splitting observations in the northern Los Angeles Basin, southern California, *Bull. seism. Soc. Am.,* **84,** 307–323.

Liu, H., Davis, P.M. & Gao, S., 1995. SKS splitting beneath southern California, *Geophys. Res. Lett.,* **22,** 767–770.

Nicholas, A.N. & Christensen, N.I.C., 1987. Formation of anisotropy in upper mantle peridotites—a review, in *Composition, Structure and Dynamics of the Lithosphere–Asthenosphere System, Geodyn. Ser.,* Vol. 16, pp. 111–123, eds Fuchs, K. & Froidevaux, C., AGU, Washington, DC.

Ozalaybey, S. & Savage, M.K., 1994. Double-layer anisotropy resolved from *S* phases, *Geophys. J. Int.,* **117,** 653–664.

Ozalaybey, S. & Savage, M.K., 1995. Shear wave splitting beneath western United States in relation to plate tectonics, *J. geophys. Res.,* **100,** 18 135–18 149.

Raikes, S.A., 1978. The temporal variation of tele-seismic *P*-residuals in southern California, *Bull. seism. Soc. Am.,* **68,** 711–720.

Ribe, N.M., 1989. Seismic anisotropy and mantle flow, *J. geophys. Res.,* **94,** 4213–4223.

Rümpker, G. & Silver, P.G., 1998. Apparent shear-wave splitting parameters in the presence of vertically varying anisotropy, *Geophys. J. Int.* **135,** 790–800.

Savage, M.K. & Silver, P.G., 1993. Mantle deformation and tectonics: constraints from seismic anisotropy in western United States, *Phys. Earth planet. Inter.,* **78,** 207–228.

Savage, M.K., Silver, P.G. & Meyer, R.P., 1990. Observations of teleseismic shear-wave splitting in the basin and range from portable and permanent stations, *Geophys. Res. Lett.,* **17,** 21–24.

Silver, P.G., 1996. Seismic anisotropy beneath the continents: probing the depths of geology, *Ann. Rev. Earth planet Sci.,* **24,** 385.

Silver, P.G. & Chan, W.W., 1991. Shear wave splitting and subcontinental mantle deformation, *J. geophys. Res.,* **96,** 16 429–16 545.

Silver, P.G. & Savage, M.K., 1994. The interpretation of shear-wave splitting parameters in the presence of two anisotropic layers, *Geophys. J. Int.* **119,** 949–963.

World Stress Map, 1997. http://www-gpi.physik.uni-karlsruhe.de/pub/wsm.

Zhang, S. & Karato, S., 1995. Lattice preferred orientation of olivine aggregates deformed in simple shear, *Nature,* **375,** 774–777.

APPENDIX A: DETAILED MAPS OF SPLITTING MEASUREMENTS

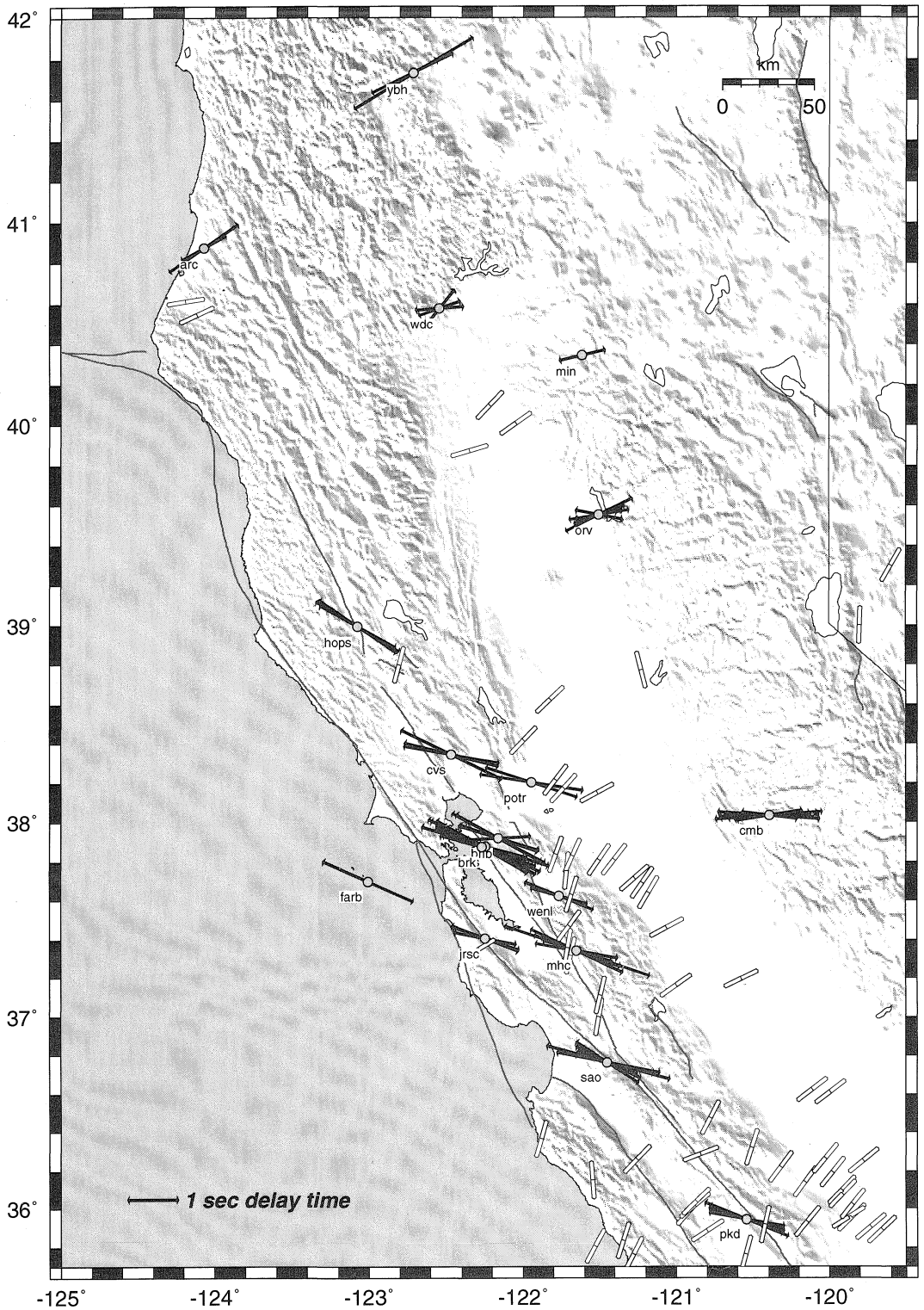

Figure A1. Northern and central California splitting measurements and WSM stress indicators. Stars indicate stations of the TriNet network, circles Berkeley network, triangles USNSN network and the squares show the Anza network stations. Other symbols as in Fig. 6.

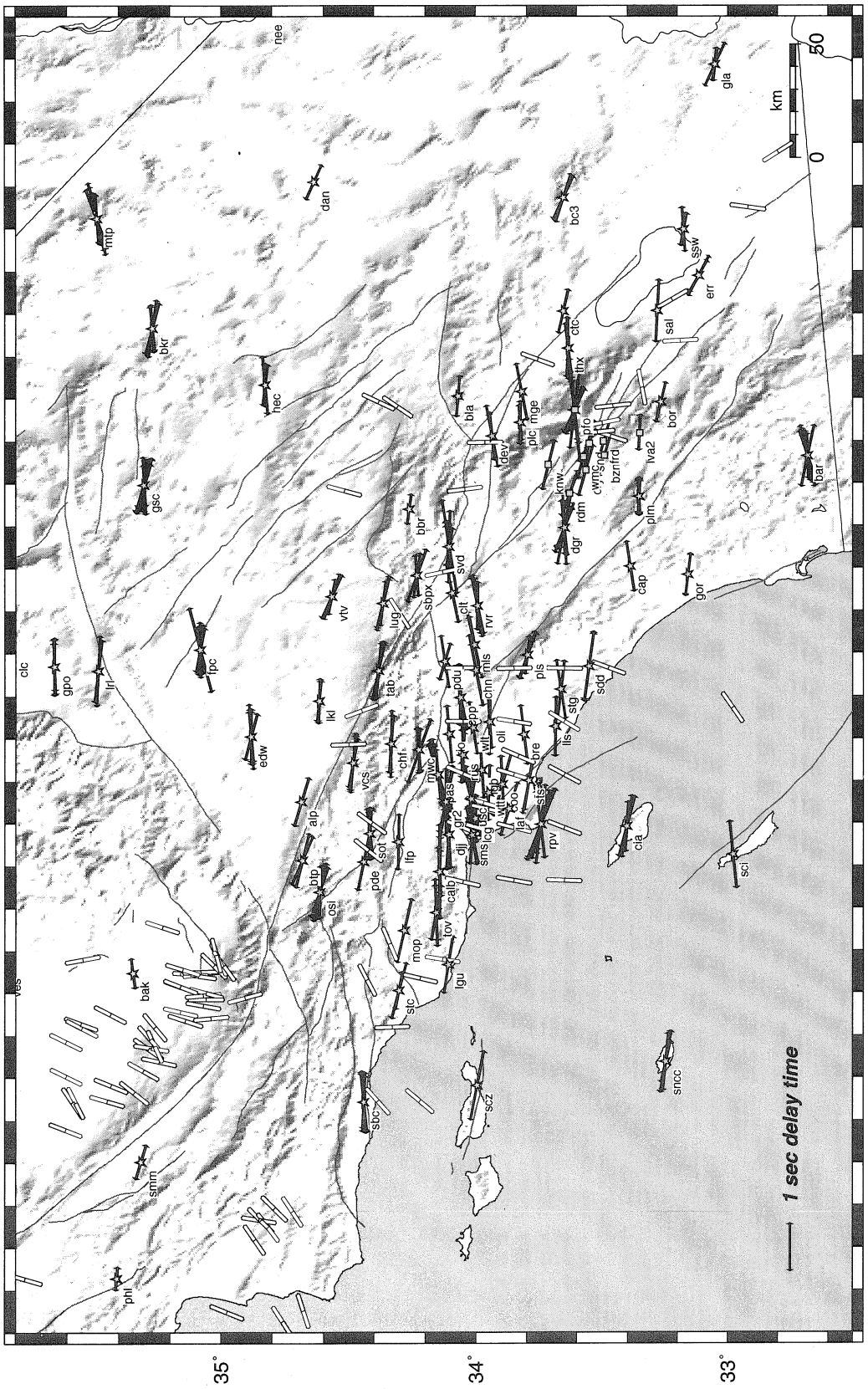

Figure A2. Southern California splitting measurements and WSM stress indicators. Symbols as in Fig. A1.

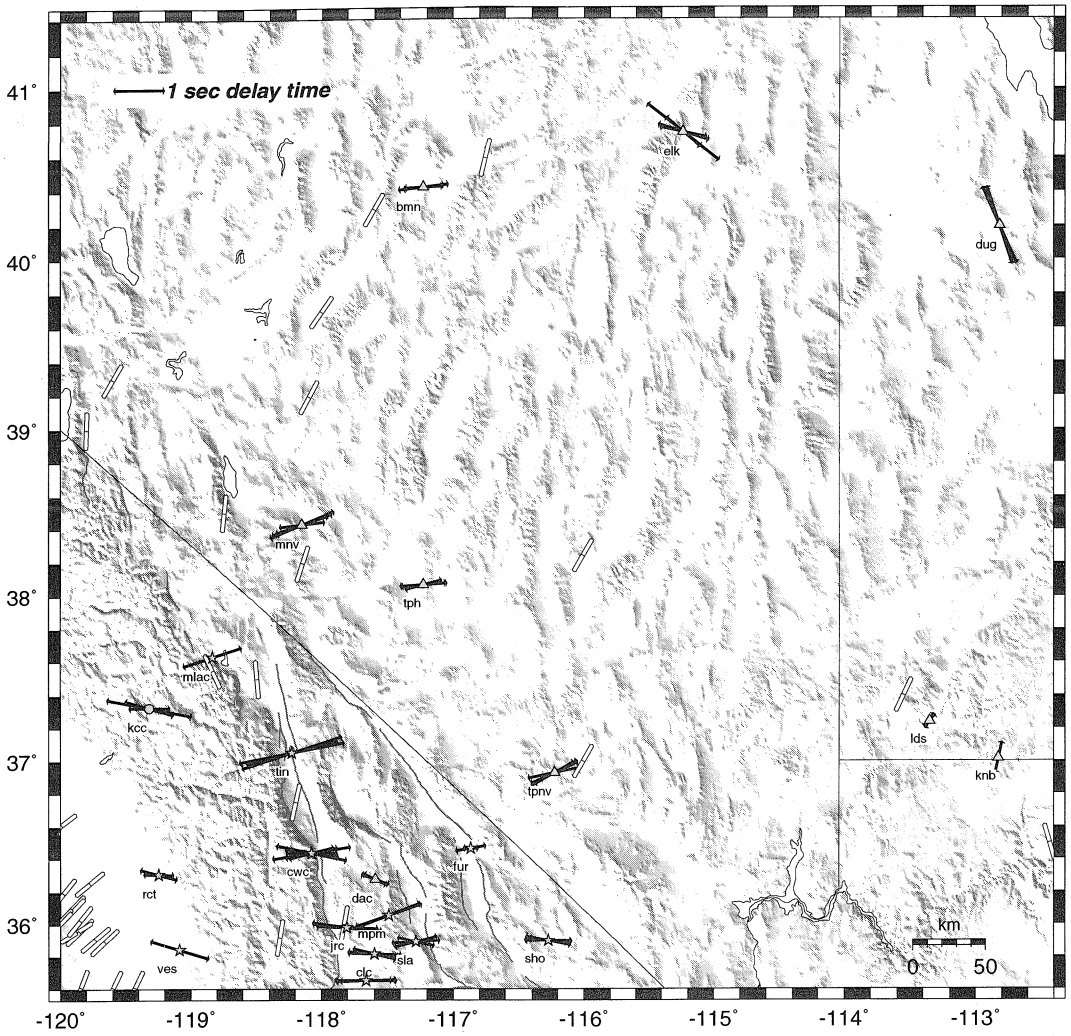

Figure A3. Eastern splitting measurements and WSM stress indicators. Symbols as in Fig. A1.